

Reduced-order model for dynamical structures having numerous local modes in the low frequency range

A. Arnoux, Anas Batou, Christian Soize, L. Gagliardini

► **To cite this version:**

A. Arnoux, Anas Batou, Christian Soize, L. Gagliardini. Reduced-order model for dynamical structures having numerous local modes in the low frequency range. 8th International Conference on Structural Dynamics, EURO-DYN 2011, KU Leuven, Jul 2011, Leuven, Belgium. pp.ISBN 978-90-760-1931-4, Pages: 2609-2614. hal-00692997

HAL Id: hal-00692997

<https://hal-upec-upem.archives-ouvertes.fr/hal-00692997>

Submitted on 1 May 2012

HAL is a multi-disciplinary open access archive for the deposit and dissemination of scientific research documents, whether they are published or not. The documents may come from teaching and research institutions in France or abroad, or from public or private research centers.

L'archive ouverte pluridisciplinaire **HAL**, est destinée au dépôt et à la diffusion de documents scientifiques de niveau recherche, publiés ou non, émanant des établissements d'enseignement et de recherche français ou étrangers, des laboratoires publics ou privés.

Reduced-order model for dynamical structures having numerous local modes in the low-frequency range.

A. Arnoux^{1,2}, A. Batou¹, C. Soize¹, L. Gagliardini²

¹Université Paris-Est, Laboratoire Modélisation et Simulation Multi-Echelle, MSME UMR 8208 CNRS, 5 Boulevard Descartes, 77454 Marne-la Vallée, France

²PSA Peugeot Citroën, Direction Technique et Industrielle, Centre Technique de Vélizy A, Route de Gisy, 78140 Vélizy Villacoublay, France
email: adrien.arnoux@univ-paris-est.fr

ABSTRACT: An automotive vehicle is made up of stiff parts and flexible components. This type of structure is characterized by the fact that it exhibits, in the low-frequency range, not only the classical global elastic modes but also numerous local elastic modes which cannot easily be separated from the global elastic modes. To solve this difficult problem, a new approach has recently been proposed to construct a reduced-order computational dynamical model. The construction of such a reduced-order computational model requires to decompose the domain into subdomains for which their mean sizes are controlled. Such a decomposition must be carried out with a general and automatic method which can be applied for very complex computational model related to complex geometry such as the computational dynamical model of an automotive vehicle. In this paper, we propose to use the Fast Marching Method for the construction of such subdomains. Nevertheless, in order to explain why such a construction has to be performed, we recall, in a first part, the method to construct the reduced-order model. Then, we present the Fast Marching Method. Finally, we present two applications, one for a simple dynamical system and another one concerning an automotive vehicle.

KEY WORDS: reduced-order model; vibroacoustics; global elastic modes; local elastic modes; Fast Marching Method.

1 INTRODUCTION

This research is performed in the context of the vibroacoustic analysis of automotive vehicles. An automotive vehicle is made up of stiff parts and flexible components. In the low-frequency range, this type of structure is characterized by the fact that it exhibits, not only the classical global elastic modes, but also numerous local elastic modes in the same low-frequency band. The problem is that in such a complex heterogeneous structure, the global elastic modes cannot clearly be separated from the local elastic modes because there are many small contributions of the local deformations in the deformations of the global elastic modes and conversely. Since there are local elastic modes in the low-frequency band, a part of the mechanical energy is transferred from the global elastic modes to the local elastic modes which store this energy and then what induces an apparent damping at the resonances associated with the global elastic modes. In order to construct a reduced-order model for the low-frequency band, which allows a good approximation of the global displacements to be predicted and then, if needed, to take into account the effects of the local displacements in the total response, a new approach [1] has recently been proposed. This method allows a basis of the global displacements and a basis of the local displacements to be calculated by solving two separated eigenvalue problems, but requires to decompose the computational model in subdomains whose sizes are controlled. In this paper, we propose to use the Fast Marching Method for the construction of such subdomains. Nevertheless, in order to explain why such a construction has to be performed, we recall, in a first part, the method to construct the reduced-order

model. Then, we present the Fast Marching Method (see [2]) which allows a front to be propagated on a complex mesh of a computational model. We present two applications, one for a simple dynamical system and another one concerning an automotive vehicle.

2 DESCRIPTION OF THE METHOD

In this section, we summarize the method introduced in [1]. This method allows a basis of the global displacements and a basis of the local displacements to be constructed by solving two separated eigenvalue problems. It should be noted that these two basis are not made up of the elastic modes. The method is based on the construction of a projection operator to reduce the kinetic energy while the elastic energy remain exact. This method is applied on the structural part of the vibroacoustic structures we are interested in.

2.1 Reference reduced model

We are interested in predicting the frequency response functions of a vibroacoustic damped structure occupying a bounded domain Ω , in the frequency band of analysis $\mathcal{B} = [\omega_{\min}, \omega_{\max}]$ with $0 < \omega_{\min}$. Let $\mathbb{U}(\omega)$ be the complex vector of the m DOF of the structural part of the vibroacoustic computational model constructed by the finite element method. Let $[\mathbb{M}]$ and $[\mathbb{K}]$ be the positive-definite symmetric $(m \times m)$ real mass and stiffness matrices. The eigenfrequencies λ and the elastic modes φ in \mathbb{R}^m of the conservative part of the dynamical computational model of the structure are the solution of the following eigenvalue

problem,

$$[\mathbb{K}] \varphi = \lambda [\mathbb{M}] \varphi. \quad (1)$$

Then an approximation $\mathbb{U}_n(\omega)$ at order n of $\mathbb{U}(\omega)$ can be written as

$$\mathbb{U}_n(\omega) = \sum_{\alpha=1}^n q_{\alpha}(\omega) \varphi_{\alpha} = [\Phi] q(\omega), \quad (2)$$

in which $q = (q_1, \dots, q_n)$ is the complex vector of the n generalized coordinates and where $[\Phi] = [\varphi_1 \dots \varphi_n]$ is the $(m \times n)$ real matrix of the elastic modes associated with the n first eigenvalues.

2.2 Decomposition of the mass matrix.

In this section, we introduce a decomposition of the mass matrix which is adapted to the calculation of the global elastic modes in the low-frequency band of analysis in which there are also a large number of local elastic modes. The details of the methodology for the discrete and the continuous cases are presented in [1].

2.2.1 Decomposition of domain Ω

Domain Ω is partitioned into n_J subdomains Ω_j^{ε} such that, for j and k in $\{1, \dots, n_J\}$,

$$\Omega = \bigcup_{j=1}^{n_J} \Omega_j^{\varepsilon}, \quad \Omega_j^{\varepsilon} \cap \Omega_k^{\varepsilon} = \emptyset. \quad (3)$$

The parameter ε is the characteristic length of the subdomains. The choice of ε is related to the smallest "wavelength" of the global elastic modes that we want to extract in presence of numerous local modes. The construction of the subdomains are presented in Section 3.

2.2.2 Projection operator

Let $u \mapsto h_{\varepsilon}^r(u)$ be the linear operator defined by

$$\{h_{\varepsilon}^r(u)\}(x) = \sum_{j=1}^{n_J} \mathbb{1}_{\Omega_j^{\varepsilon}}(x) \frac{1}{m_j} \int_{\Omega_j^{\varepsilon}} \rho(x) u(x) dx, \quad (4)$$

in which $x \mapsto \mathbb{1}_{\Omega_j^{\varepsilon}}(x) = 1$ if x is in Ω_j^{ε} and $= 0$ otherwise.

The local mass m_j is defined, for all j in $\{1, \dots, n_J\}$, by $m_j = \int_{\Omega_j^{\varepsilon}} \rho(x) dx$, where $x \mapsto \rho(x)$ is the mass density. Let $u \mapsto h_{\varepsilon}^c(u)$ be the linear operator defined by

$$h_{\varepsilon}^c(u) = u - h_{\varepsilon}^r(u). \quad (5)$$

Function $h_{\varepsilon}^r(u)$ will also be denoted by u^r and function $h_{\varepsilon}^c(u)$ by u^c . We then have $u = h_{\varepsilon}^r(u) + h_{\varepsilon}^c(u)$ that is to say, $u = u^r + u^c$. Let $[H_{\varepsilon}^r]$ be the $(m \times m)$ matrix relative to the finite element discretization of the projection operator h_{ε}^r defined by Eq. (4). Therefore, the finite element discretization \mathbb{U} of u can be written as $\mathbb{U} = \mathbb{U}^r + \mathbb{U}^c$, in which

$$\mathbb{U}^r = [H_{\varepsilon}^r] \mathbb{U}$$

and

$$\mathbb{U}^c = [H_{\varepsilon}^c] \mathbb{U} = \mathbb{U} - \mathbb{U}^r,$$

which shows that $[H_{\varepsilon}^c] = [I_m] - [H_{\varepsilon}^r]$. Then, the reduced $(m \times m)$ mass matrix $[\mathbb{M}^r]$ is such that

$$[\mathbb{M}^r] = [H_{\varepsilon}^r]^T [\mathbb{M}] [H_{\varepsilon}^r],$$

and the complementary $(m \times m)$ mass matrix $[\mathbb{M}^c]$ is such that

$$[\mathbb{M}^c] = [H_{\varepsilon}^c]^T [\mathbb{M}] [H_{\varepsilon}^c].$$

Using the properties of the projection operator defined by Eq. (4), it can be shown [1] that

$$[\mathbb{M}^c] = [\mathbb{M}] - [\mathbb{M}^r].$$

2.3 Global and local displacements bases

As proposed in [1], two methods are proposed to calculate the global displacements basis and the local displacements basis that will be used to reduce the matrix equation.

2.3.1 Direct method

In such a method, the basis of the global displacements and the basis of the local displacements are directly calculated using the decomposition of the mass matrix $[\mathbb{M}]$. The global displacements eigenvectors ϕ^g in \mathbb{R}^m are solution of the following generalized eigenvalue problem

$$[\mathbb{K}] \phi^g = \lambda^g [\mathbb{M}^r] \phi^g. \quad (6)$$

This generalized eigenvalue problem admits an increasing sequence of $3n_J$ positive eigenvalues $0 < \lambda_1^g \leq \dots \leq \lambda_{3n_J}^g$, associated with the finite family of algebraically independent vectors $\{\phi_1^g, \dots, \phi_{3n_J}^g\}$. The family $\{\phi_1^g, \dots, \phi_{3n_J}^g\}$ is defined as the family of the global displacements eigenvectors and these vectors do generally not belong to the family of the elastic modes. The local displacements eigenvectors ϕ^l in \mathbb{R}^m are solution of the generalized eigenvalue problem

$$[\mathbb{K}] \phi^l = \lambda^l [\mathbb{M}^c] \phi^l. \quad (7)$$

This generalized eigenvalue problem admits an increasing sequence of positive eigenvalues $0 < \lambda_1^l \leq \dots \leq \lambda_{m-3n_J}^l$, associated with the finite family of vectors $\{\phi_1^l, \dots, \phi_{m-3n_J}^l\}$. The family $\{\phi_1^l, \dots, \phi_{m-3n_J}^l\}$ is defined as the family of the local displacements eigenvectors and do generally not belong to the family of the elastic modes. Matrices $[\mathbb{M}^r]$ and $[\mathbb{M}^c]$ are symmetric and positive but are not positive definite (positive semi-definite matrices). The rank of matrices $[\mathbb{M}^r]$ and $[\mathbb{M}^c]$ are n_J and $m - 3n_J$ respectively.

2.3.2 Double projection method

This method is less intrusive with respect to the commercial software and less time-consuming than the direct method. The solutions of the generalized eigenvalue problems defined by Eqs. (6) and (7) are then written, for n sufficiently large, as

$$\phi^g = [\Phi] \tilde{\phi}^g, \quad \phi^l = [\Phi] \tilde{\phi}^l, \quad (8)$$

in which $[\Phi]$ defined in Eq. (2) is the matrix of the elastic modes. The global displacements eigenvectors are the solutions of the

generalized eigenvalue problem

$$[\tilde{K}] \tilde{\phi}^g = \lambda^g [\tilde{M}^r] \tilde{\phi}^g, \quad (9)$$

in which $[\tilde{M}^r] = [\Phi_\varepsilon^r]^T [\mathbb{M}] [\Phi_\varepsilon^r]$ and $[\tilde{K}] = [\Phi]^T [\mathbb{K}] [\Phi]$, and where the $(m \times n)$ real matrix $[\Phi_\varepsilon^r]$ is such that $[\Phi_\varepsilon^r] = [H_\varepsilon^r] [\Phi]$. The local displacements eigenvectors are the solutions of the generalized eigenvalue problem

$$[\tilde{K}] \tilde{\phi}^\ell = \lambda^\ell [\tilde{M}^c] \tilde{\phi}^\ell, \quad (10)$$

in which $[\tilde{M}^c] = [\Phi_\varepsilon^c]^T [\mathbb{M}] [\Phi_\varepsilon^c]$ and where the $(m \times n)$ real matrix $[\Phi_\varepsilon^c]$ is such that $[\Phi_\varepsilon^c] = [H_\varepsilon^c] [\Phi] = [\Phi] - [\Phi_\varepsilon^r]$.

2.4 Mean reduced model

It is proven in [1] that the family $\{\phi_1^g, \dots, \phi_{3n_j}^g, \phi_1^\ell, \dots, \phi_{m-3n_j}^\ell\}$ is a basis of \mathbb{R}^m . The mean reduced matrix model is obtained by the projection of $\mathbb{U}(\omega)$ on the family $\{\phi_1^g, \dots, \phi_{n_g}^g, \phi_1^\ell, \dots, \phi_{n_\ell}^\ell\}$ of real vectors associated with the n_g first global displacements eigenvectors such that $n_g \leq 3n_j \leq m$ and with the n_ℓ first local displacements eigenvectors such that $n_\ell \leq m$. It should be noted that, if the double projection method is used, then we must have $n_g \leq n$, $n_\ell \leq n$ and $n_t \leq n$ in which $n_t = n_g + n_\ell$. Then, the approximation $\mathbb{U}_{n_g, n_\ell}(\omega)$ of $\mathbb{U}(\omega)$ at order (n_g, n_ℓ) is written as

$$\mathbb{U}_{n_g, n_\ell}(\omega) = \sum_{\alpha=1}^{n_g} q_\alpha^g(\omega) \phi_\alpha^g + \sum_{\beta=1}^{n_\ell} q_\beta^\ell(\omega) \phi_\beta^\ell. \quad (11)$$

3 CONSTRUCTION OF THE SUBDOMAINS

For the computational model of a complex structure such as an automotive vehicle, the decomposition of the domain is not easy to be carried out because the geometry is very complex and curved. The method we propose for this decomposition is based on the Fast Marching Methods (FMM) introduced in [2] which gives a way to propagate a front (the notion of front will be defined below) on connected parts from a starting point. In this section, the FMM is summarized and then we explain how to construct the subdomains using the FMM.

3.1 Presentation of the Fast Marching Method (FMM)

Let \mathbf{x} be the generic point in \mathbb{R}^3 belonging to the complex geometry Ω . Let \mathbf{x}_0 be a fixed point belonging to Ω . Let $U(\mathbf{x})$ be a geodesic distance adapted to the geometry, between \mathbf{x} and \mathbf{x}_0 . It should be noted that for a simple 3D volume domain, such a geodesic distance would be the Euclidean distance $\|\mathbf{x} - \mathbf{x}_0\|$ in which $\|\cdot\|$ is the Euclidean norm. The front related to \mathbf{x}_0 is defined as the subset of all the \mathbf{x} such that $U(\mathbf{x})$ has a fixed value. The FMM [2] allows the front to be propagated from starting point \mathbf{x}_0 . We then have to calculate $U(\mathbf{x})$ verifying the following nonlinear Eikonal equation

$$\|\nabla U(\mathbf{x})\| = F(\mathbf{x}), \quad \mathbf{x} \in \Omega, \quad (12)$$

with ∇ the gradient with respect to \mathbf{x} , in which $F(\mathbf{x})$ is a given arbitrary positive-valued function and for which the boundary condition is written as $U(\mathbf{x}) = 0$ on Γ_0 which is a curved line or a surface containing \mathbf{x}_0 . Introducing the finite element mesh of Ω ,

Eq. (12) is discretized using an *upwind* approximation (forward finite difference) for the gradient (see [2]). For the particular case of a rectangular regular finite element mesh for which the mesh size is h and for which the nodes are \mathbf{x}_{ij} , we have to find $U_{ij} = U(\mathbf{x}_{ij})$ as the solution of the following equation

$$\begin{aligned} & \{\max(U_{ij} - U_{i-1,j}, U_{ij} - U_{i+1,j}, 0)\}^2 \\ & + \{\max(U_{ij} - U_{i,j-1}, U_{ij} - U_{i,j+1}, 0)\}^2 = h^2 F_{ij}^2. \end{aligned} \quad (13)$$

Since the information in Eq. (13) propagates in a unique way, this equation allows the front to be propagated from the starting point. The use of the word *Fast* in FMM is due to the fact that the nodes associated with U_{ij} and identified by Eq. (13) belong to a small domain which is called the Narrow Band (NB).

- In the FMM, the algorithm introduces three groups of nodes:
- (1) *alive* nodes for which the value of U_{ij} is fixed and does not change,
 - (2) *trial* nodes for which the value of U_{ij} is given but has to be updated until they become *alive* and these nodes constitute the Narrow Band,
 - (3) *far* nodes which have not been reached by the front and therefore are such that $U_{ij} = +\infty$.

The front is propagated using the following algorithm:

Initialization

- Choose a starting node \mathbf{x}_0 rewritten as $\mathbf{x}_{0,0}$, which is *alive* and set $U_{0,0} = U(\mathbf{x}_{0,0}) = 0$.
- The 4 neighboring nodes of $\mathbf{x}_{0,0}$ become *trial* nodes and the associated value of U is set to hF_{ij} .
- All the other nodes are *far* nodes with associated value of U equal to infinity.

Loop

- Search among *trial* nodes, the node \mathbf{x}_{ij} with the smallest value of U .
- Remove \mathbf{x}_{ij} from *trial* nodes and add \mathbf{x}_{ij} to *alive* nodes.
- For each neighboring node of \mathbf{x}_{ij} , there are two possible cases:
 - if the neighboring node is a *far* node, add it to the *trial* nodes and its value of U is set to $U_{ij} + hF_{ij}$.
 - if the neighboring node is a *trial* node, its value of U is updated solving Eq. (13).

The Loop is repeated until all the node are *alive*.

3.2 Extension to a triangular mesh

For triangular meshes, the algorithm described above is unchanged but Eq. (13) must be adapted. We consider the case represented in Fig. 2 for which the value $U_c = U(\mathbf{x}_c)$ of the node \mathbf{x}_c has to be updated using the value $U_a = U(\mathbf{x}_a)$ of the node \mathbf{x}_a and the value $U_b = U(\mathbf{x}_b)$ of the node \mathbf{x}_b which are *alive* nodes. We then obtain the following equation [2]

$$(\mathbf{a}^T [Q] \mathbf{a}) U_c^2 + (2\mathbf{a}^T [Q] \mathbf{b}) U_c + (\mathbf{b}^T [Q] \mathbf{b}) = F_c^2, \quad (14)$$

in which $\mathbf{a} = (1, 1)$, $\mathbf{b} = (-U_a, -U_b)$ and where the matrix $[Q]$ is written as $[Q] = [P][P]^T$ in which the matrix $[P]$ is defined by

$$[P] = \begin{bmatrix} x_c - x_a & x_c - x_b \\ y_c - y_a & y_c - y_b \\ z_c - z_a & z_c - z_b \end{bmatrix}, \quad (15)$$

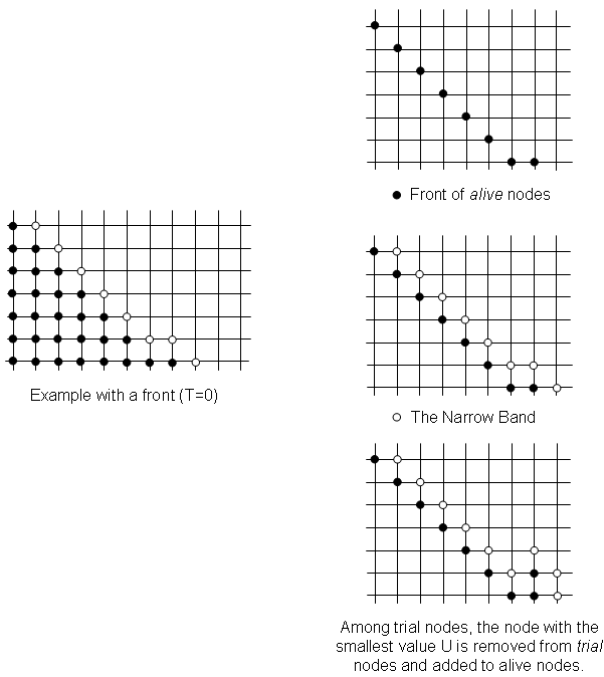


Figure 1. Diagram of the Fast Marching Method

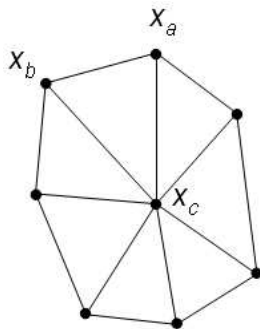


Figure 2. Triangular mesh (with acute angle) around node \mathbf{x}_c .

in which (x_a, y_a, z_a) , (x_b, y_b, z_b) and (x_c, y_c, z_c) are the coordinates of points \mathbf{x}_a , \mathbf{x}_b and \mathbf{x}_c . It can be shown [2] that Eq. 14 admits two positive solutions if the angle $\widehat{\mathbf{x}_a \mathbf{x}_c \mathbf{x}_b}$ is acute. If the mesh contains obtuse angles, then the method has to be adapted using the unfolding step presented in [3].

3.3 Construction of the subdomains

The subdomains Ω_j^ε of Ω are constructed using the FMM. This construction has two steps. The first one consists in finding the centers of the subdomains. The second one consists in generating the subdomains using these centers as starting points.

(i) Computation of the subdomains centers

The algorithm is the following:

Initialization

- Choose a value for parameter ε .
- Choose a first centre $\mathbf{x}_{0,0}^1$.

Loop

- Set the center $\mathbf{x}_{0,0}^j$ as the starting point of the FMM and propagate the front.
- Stop the front when the value of U of the last *alive* node is greater than ε .
- Set this last *alive* node as the center $\mathbf{x}_{0,0}^{j+1}$ and set all the *alive* nodes as ineligible nodes to be a center.

This algorithm allows a homogeneous spatial repartition of the centers to be constructed.

(ii) Computation of the subdomains

To construct the subdomains Ω_j^ε using a set of centers $\mathbf{x}_{0,0}^j$, we simultaneously propagate a front starting from each center until all the nodes become *alive* nodes with respect to one of the front. Then, the boundaries of the subdomains correspond to the meeting lines of the fronts.

4 APPLICATION

In this section, we present two applications of the methodology presented in the previous sections. The first one is a simple structure which has previously been presented in [1] and the second one is relative to a real automotive model.

4.1 First application

The system is made up of 12 flexible panels and a stiff structure (see Fig. 3). For the flexible parts, all panels are rectangular $4 m \times 4 m$, homogeneous, isotropic, with constant thickness $0.002 m$, mass density equal to $7.8 kg/m^3$ and Poisson ratio equal to 0.29. Moreover, the Young modulus is different for all the panels. The stiff structure is homogeneous, isotropic, with constant thickness $0.017 m$, mass density equal to $9.8 kg/m^3$, Poisson ratio equal to 0.29 and the Young modulus is $2.1 \times 10^{12} N/m^2$. The frequency band of analysis is $B =]0, 11] Hz$. The structure has 13 014 DOF.

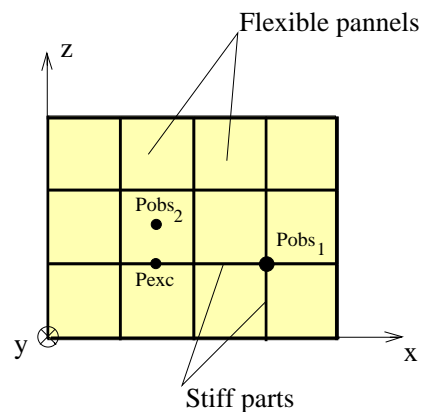


Figure 3. The dynamical system

4.1.1 Decomposition of the domain

The FMM method presented in Section 3 is applied to the mesh of the structure with $\varepsilon = 3 m$. The centers of the subdomains are represented in Fig. 4 and the subdomains obtained from these centers are represented in Fig. 5.

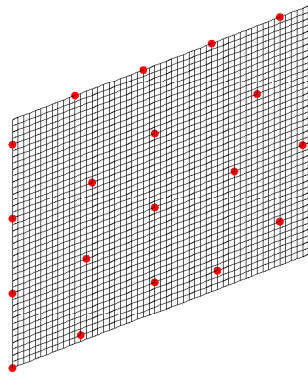


Figure 4. Centers of the subdomains

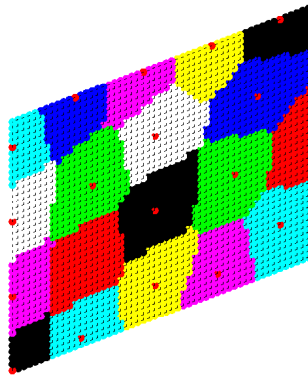
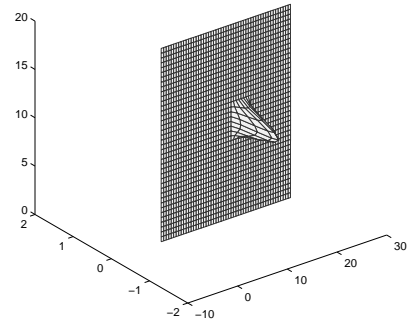


Figure 5. Subdomains

Mode 1 - 1.6722 Hz



Mode 2 - 1.8204 Hz

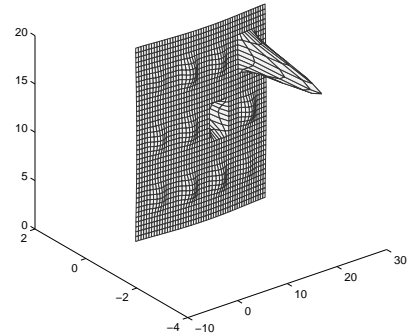


Figure 6. First elastic mode (top) and second elastic mode (down).

4.1.2 Elastic modes, global and local displacements eigenvectors

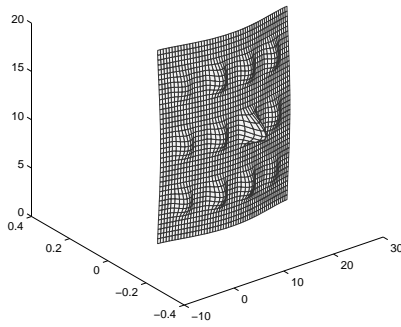
In a first step, the elastic modes are calculated with the finite element model. There are 86 eigenfrequencies in the frequency band of analysis B and $n = 120$ eigenfrequencies in the frequency band $]0, 13.2] Hz$. The first elastic mode ϕ_1 and the second elastic mode ϕ_2 are displayed in Fig. 6 which shows that ϕ_1 is a local elastic mode while ϕ_2 is a global elastic mode with an important local displacement. In a second step, the global and local displacements eigenvectors are constructed using the double projection method. In frequency band $]0, 13.2] Hz$, there are $n_g = 8$ global displacements eigenvectors and $n_\ell = 112$ local displacements eigenvectors. The first two global displacements eigenvectors ϕ_1^g, ϕ_2^g and the first two local displacements eigenvectors ϕ_1^l and ϕ_2^l are shown in Fig. 7.

4.2 Frequency responses functions

For all $\omega \in B$, the structure is subjected to an external point load equal to 1 N applied to the node Pexc whose coordinates are (10,0,7) located in the stiff part. The mean damping matrix is constructed using a Rayleigh model corresponding to a damping rate $\xi = 0.04$ for the eigenfrequency $f_1 = 1.67 Hz$ and for the eigenfrequency $f_{120} = 13.2 Hz$. The response is

calculated at two observation points, the point Pobs₁ located in the stiff part at the node whose coordinates are (19,0,7) and the point Pobs₂ located in the flexible part at the node whose coordinates are (10,0,10) (see Fig. 3). The response is calculated for different projections associated with the different bases: for the elastic modes ($n = 120$), for global displacements eigenvectors ($n_g = 8$ and $n_\ell = 0$), for local displacements eigenvectors ($n_g = 0$ and $n_\ell = 112$) and finally, for global and local displacements eigenvectors ($n_g = 8$ and $n_\ell = 112$). The moduli in log scale of the responses are displayed in Fig. 8. It can be seen that the responses calculated using global and local displacements eigenvectors are exactly the same that the response calculated using the elastic modes. For point Pobs₁ in the stiff part, the contribution of the global displacements eigenvectors is preponderant in the very low-frequency band but the contribution of the local displacements eigenvectors becomes not negligible in the high part of the low-frequency band. For point Pobs₂ in the flexible part, the contribution of the local displacements eigenvectors is important except for the first resonance corresponding to the first global displacements eigenvectors (because the flexible plates follow the stiff part in its displacement).

First global displacements eigenvector - 1.8325 Hz



First local displacements eigenvector - 1.6771 Hz

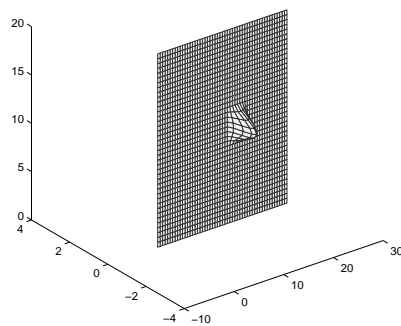


Figure 7. First global displacements eigenvector (top) and first local displacements eigenvector (bottom).

4.3 Application of the FMM to a complex geometry of an automotive vehicle

The FMM is carried out using the computational model (Finite Element Model) of the structure of an automotive vehicle. Such a FE model has 250 000 nodes and contains various types of finite elements such as volume finite elements, surface finite elements and beam elements (see Fig.9). The subdomains obtained using FMM method are represented on Fig. 10.

5 CONCLUSION

In this paper, we have presented the use of the Fast Marching Method adapted to complex geometry in order to construct the computational model subdomains which are required to implement a new methodology allowing a reduced-order computational dynamical model to be constructed in the low-frequency domain when such a low-frequency domain simultaneously contains global and local elastic modes which cannot easily be separated with usual methods.

REFERENCES

[1] C. Soize and A. Batou, Stochastic reduced-order model in low frequency dynamics in presence of numerous local elastic modes, *Journal of Applied Mechanics*, accepted in June 2010.
 [2] J.A. Sethian, A Fast Marching Level Set Method for Monotonically Advancing Fronts, *Proc. Nat. Acad. Sci.*, 93, 4, 1996.
 [3] J.A. Sethian and R. Kimmel, Computing Geodesic Paths on Manifolds A Fast Marching Level Set Method for Monotonically Advancing Fronts, *Proc. Nat. Acad. Sci.*, 95, 8431-8435, 1998.

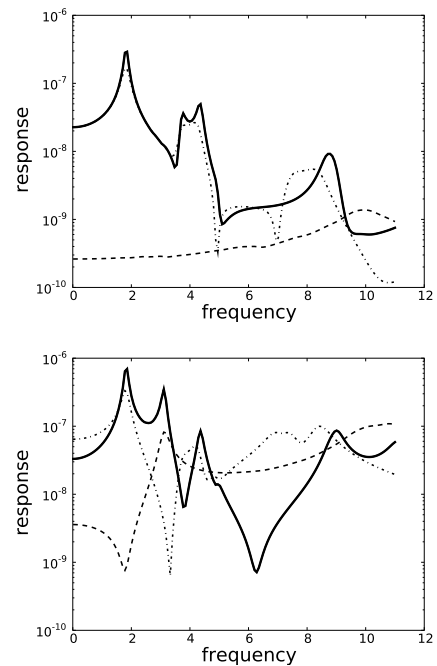


Figure 8. Modulus in log scale of the frequency response function for Pobs₁ (top) and Pobs₂ (down). Comparisons between different projection bases: elastic modes (solid thick line), global displacements eigenvectors only (mixed line), local displacements eigenvectors only (dashed line), global and local displacements eigenvectors (solid thin line superimposed to the solid thick line).

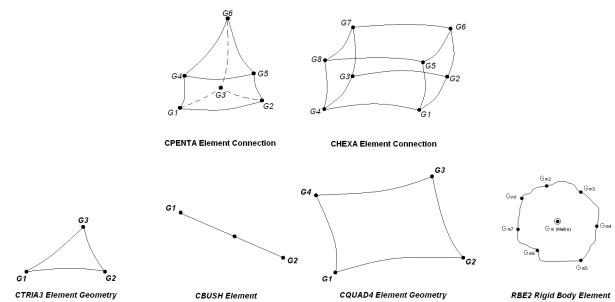


Figure 9. Diagram of the different types of finite elements

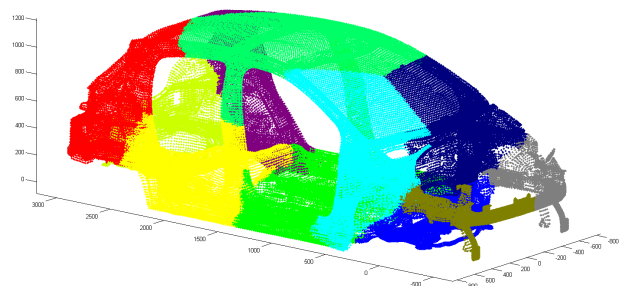


Figure 10. 12 subdomains (one per color) corresponding to 12 starting nodes for a car with an epsilon of 1.2 m